

# New method for ellipse detection by means of symmetry

Peng-Yeng Yin

Ling-Hwei Chen

National Chiao Tung University

Department of Computer and Information Science

1001 Ta Hsueh Road

Hsinchu, Taiwan 30050

---

**Abstract.** We propose a new approach for detecting ellipses. The approach is based on the geometrical property that five points on an ellipse can determine the parameters of the ellipse, and the symmetry of ellipses is used to obtain these points. Using symmetry, we classify the edge points in an input image into several subimages. Ellipses with different symmetric axes will lie in different subimages. In each subimage, symmetry is applied again to obtain those sets of five points that possibly lie on the same ellipse. Finally, using geometrical properties and the Hough transform, we extract all ellipses in an input image successfully. The proposed method can detect partially occluded ellipses. Experimental results show that the proposed method is fast and robust.

---

## 1 Introduction

The detection of elliptical shapes is an important task in computer vision. When viewed obliquely, 3-D circular profiles usually project to elliptical shapes in a 2-D image. If ellipses can be reliably detected, the parameters of the detected ellipses can be used to infer the relative orientations of objects and cameras, providing cues to interpret the 3-D world.

The Hough transform (HT)<sup>1</sup> has long been used to detect analytically defined shapes in an image. The conventional HT consists of two stages. The first stage takes pieces of evidence and votes for all parameter combinations, which are consistent with the evidence, in an accumulator array.

The second stage searches each local peak in the accumulator array and verifies the existence of the candidate shape associated with these parameters. The main advantage of HT is that it is inherently robust against partially occluded and noise-corrupted images. The major disadvantage, however, is that the computation time and the storage space required grow exponentially with the number of parameters.

Direct application of the conventional HT for ellipse detection is not practical. Because an ellipse is characterized by five parameters  $(x_0, y_0, a, b, \theta)$ , where  $(x_0, y_0)$  are the coordinates of the ellipse center,  $a$  and  $b$  are the half lengths of the major and minor axes, and  $\theta$  is the rotation angle, the resource demands become very large. Many methods have been proposed for treating this problem. Tsuji and Matsumoto<sup>2</sup> first introduced the decomposition concept by the use of the gradient. The first step is to locate ellipse centers by accumulating the midpoint of each pair of edge points with parallel tangents. The next step is to use a geometric property for selecting candidates that are exactly on the ellipse. The final step is to evaluate the five parameters of the ellipse that best fit these candidates by the mean least squares method. The proposed center-finding process will not work if the number of symmetric pairs of points about the ellipse center is too small. Tsukune and Goto<sup>3</sup> used the same center-finding process previously mentioned and obtained the remaining parameters by multiplying the polynomial form of parameterization by two. Ballard<sup>4</sup> presented a method that simplifies the parameterization by deriving the ellipse center  $(x_0, y_0)$  from  $x_i, y_i, a, b, \theta$ , and  $dY/dX$ , where  $(x_i, y_i)$  are the coordinates of the edge pixel and  $dY/dX$  is the tangent at that pixel. Yuen, Illingworth, and Kittler<sup>5</sup> proposed a better

---

Paper 93-026 received May 5, 1993; revised manuscript received Oct. 25, 1993; accepted for publication Nov. 11, 1993.  
1017-9909/94/\$6.00. © 1994 SPIE and IS&T.

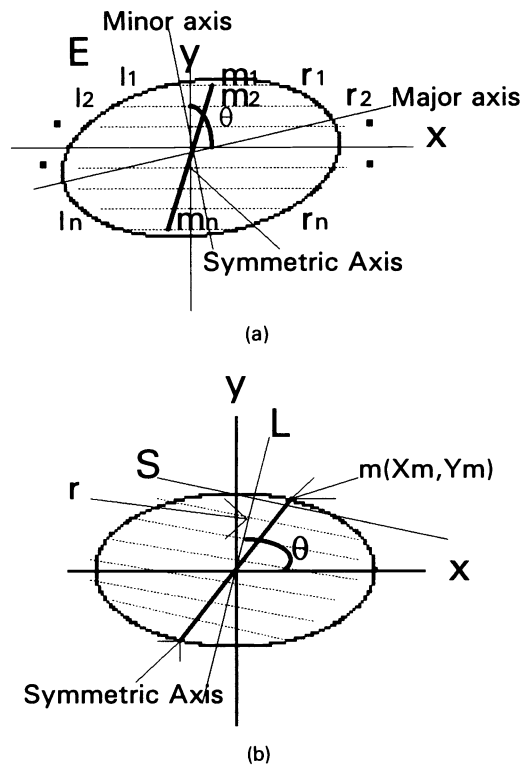


**Fig. 1** The symmetric property for an ellipse. (a) Ellipse  $E$  is scanned from left to right and top to bottom. The scan lines represented by dotted lines intersect the ellipse at a sequence of pixel pairs denoted by  $(l_1, r_1), (l_2, r_2), \dots, (l_n, r_n)$ . All of the midpoints  $m_i$  of  $l_i$  and  $r_i$  for  $i$  from 1 to  $n$  lie on the same straight line. (b) The ellipse in (a) is rotated into one with the major axis along the  $x$  axis and the minor axis along the  $y$  axis.

center-finding process that employed a geometric property and then estimated the other three parameters based on the adaptive HT.<sup>6</sup> This approach can detect partially occluded ellipses better than previous ones. Huang<sup>7</sup> proposed a method that uses the duality characteristic. If the boundary points of an ellipse are taken to be the centers of other ellipses with the same major and minor axes and orientation, then those ellipses have a common boundary point on the center of the original ellipse. The gradient information is then used to reduce the voting space. More recently, Yip, Tam, and Leung<sup>8</sup> presented an approach that utilizes parallel edge points to deduce the parameters and then applies a distinguished voting rule for transforming the parameters to four special vertex positions on the corresponding ellipse. Based on the voting rule, only a 2-D array is needed for ellipse detection. All of the above-mentioned methods use the gradient information, but it is difficult to precisely estimate the gradient because of noise and quantization error. The inaccuracies of gradients affect the results of the previous methods.

In this paper, a new ellipse detector is proposed based on the geometrical property that five points on the same ellipse can determine the parameters of the ellipse. First, the detector classifies all edge points in an input image into several subimages based on the symmetry of ellipses. Ellipses with different symmetric axes will lie on different subimages. Then in each subimage, the property of symmetry is used again to locate all possible sets of five points lying on the same ellipse.

Each located set, which can produce a set of parameters of an ellipse, is considered to be a voter of this ellipse. Finally, those ellipses with many voters are taken as results. The experimental results show that the proposed method is fast and robust.

The remainder of this paper is organized as follows: Sec. 2 describes the proposed approach in detail, Sec. 3 gives experimental results, and Sec. 4 presents conclusions.

## 2 The New Approach

The conventional HT maps each edge point to a locus or a hypersurface in the parameter space. This type of transform mapping involves a large number of computations. If several edge points can be considered simultaneously, only one point in the parameter space is obtained by the characteristic function of the analytic shape. For example, two edge points can determine a straight line, three edge points can determine a circle, and five edge points can determine an ellipse, if they are all on the corresponding analytic shape. This type of transform mapping reduces the number of votes that do not come from the evidence strongly supporting the existence of the detected shape. The computational efficiency is greatly improved if the search for these critical edge points is conducted in an efficient way.

The proposed method presents an efficient search for the five edge points that determine the parameters of an ellipse. First, the edge points are classified into subimages by means of the property of symmetry—ellipses with different symmetric axes will lie in different subimages. Then, in each subimage, each set of five edge points possibly lying on an ellipse is located and the corresponding parameters of the ellipse are estimated. Finally, based on the concept of HT, all ellipses in an input image can be extracted.

### 2.1 Transformation Based on the Property of Symmetry

In this subsection, a property of symmetry for an ellipse is introduced. Based on this property, a transform procedure is presented to produce the symmetric axes for ellipses.

**Theorem.** Let an ellipse  $E$  be scanned from left to right and top to bottom [we will refer to this as a rightward scan, see Fig. 1(a)]. Let  $(l_1, r_1), (l_2, r_2), \dots, (l_n, r_n)$  shown in Fig. 1(a) be the sequence of pixel pairs generated by the scanning process. Let  $m_i$  be the midpoint of  $l_i$  and  $r_i$  for  $i$  from 1 to  $n$ . Then  $m_1, m_2, \dots, m_n$  will lie on the same straight line (which we call the *symmetric axis* of  $E$ ).

**Proof.** Without loss of generality, suppose that the origin of the coordinate system is at the center of ellipse  $E$  and the angle between the major axis of ellipse  $E$  and the  $y$  axis is  $\theta$ . We can rotate  $E$  clockwise  $(\pi/2) - \theta$  into an ellipse with the major axis along the  $x$  axis and the minor axis along the  $y$  axis [see Figs. 1(a) and 1(b)]. Then the rotated ellipse can be described by the following equation:

$$\frac{x^2}{a^2} + \frac{y^2}{b^2} = 1 \quad (1)$$

We also rotate all scan lines clockwise  $(\pi/2) - \theta$ . To obtain the general equation for all of the rotated scan lines, we draw a straight line  $L$  passing through the ellipse center and per-

pendicular to all of the rotated scan lines. It is easy to see that the straight line  $L$  makes an angle  $\theta$  with the  $x$  axis. For any rotated scan line  $S$  with a distance  $r$  to the ellipse center, the equation describing  $S$  can be represented as

$$x \cos\theta + y \sin\theta = r \quad (2)$$

Let  $S$  intersect  $E$  at two points  $(x_1, y_1)$  and  $(x_2, y_2)$ , and let the midpoint of these two points be  $m(x_m, y_m)$ . Then  $(x_m, y_m)$  can be derived by solving Eqs. (1) and (2). From Eq. (2), we have

$$x = \frac{r - y \sin\theta}{\cos\theta} \quad (3)$$

Substituting Eq. (3) into Eq. (1), we obtain

$$(a^2 \cos^2\theta + b^2 \sin^2\theta)y^2 - (2rb^2 \sin\theta)y + r^2b^2 - a^2b^2 \cos^2\theta = 0 \quad (4)$$

Because the two roots of Eq. (4) are  $y_1$  and  $y_2$ , and  $y_m$  is the average of  $y_1$  and  $y_2$ , we can determine  $y_m$  as follows:

$$y_m = \frac{y_1 + y_2}{2} = \frac{rb^2 \sin\theta}{a^2 \cos^2\theta + b^2 \sin^2\theta} \quad (5)$$

Similarly, from Eq. (2), we have

$$y = \frac{r - x \cos\theta}{\sin\theta} \quad (6)$$

Substituting Eq. (6) in Eq. (1), we obtain

$$(a^2 \cos^2\theta + b^2 \sin^2\theta)x^2 - (2ra^2 \cos\theta)x + r^2a^2 - a^2b^2 \sin^2\theta = 0 \quad (7)$$

Then  $x_m$  can be determined by the two roots  $x_1$  and  $x_2$  of Eq. (7) and can be expressed as

$$x_m = \frac{x_1 + x_2}{2} = \frac{ra^2 \cos\theta}{a^2 \cos^2\theta + b^2 \sin^2\theta} \quad (8)$$

Finally, the tangent  $t_m$  of the midpoint  $m$  can be computed to be

$$t_m = \frac{y_m}{x_m} = \frac{b^2 \sin\theta}{a^2 \cos\theta} \quad (9)$$

which is a constant. That is, all of the midpoints  $m_1, m_2, \dots, m_n$  lie on the same line that passes through the ellipse center and with the tangent  $b^2 \sin\theta/a^2 \cos\theta$ , which proves the theorem.

We now refer to the property that all mid points  $m_1, m_2, \dots, m_n$  lie on the same line as the property of symmetry and up to the same line as the symmetric axis of the ellipse. The same property holds when the ellipse is scanned from top to bottom and left to right (i.e., downward).

Let  $f$  be an input image with size  $n \times n$  and  $F$  be the binary result of the edge-extracted image from  $f$ , with 1 representing a black point and 0 a white point. Based on the property of symmetry,  $F$  is scanned rightward and the ellipses in  $F$  can be transformed to the corresponding symmetric axes by the following procedure.

### The transform procedure:

```

/* To transform the ellipses in the input image F to their */
/* corresponding symmetric axes in the resulting image G */
For i = 1 to n/* from top to bottom */
  For j = 1 to n/* from left to right */
    G(i, j) = 0; /* to clear image G */
  For i = 1 to n/* from top to bottom */
    For j = 1 to n/* from left to right */
      If (F(i, j) = 1) then /* the scan line meets an edge point
        (i, j) */
        For k = j + 1 to n
          If (F(i, k) = 1) then /* the scan line meets another
            edge point (i, k) */
            G(i, (j+k)/2) = 1; /* keep the midpoint of (i, j) and
              (i, k) in the image G */

```

The merit of this type of transformation from ellipses to straight lines is that the ellipses can be classified into several subimages according to their symmetric axes, and ellipses with different symmetric axes will lie in different subimages. This classification greatly simplifies later tasks.

The classification procedure is described next.

## 2.2 Classification

Although five distinct points on an ellipse can determine the parameters of the ellipse, an exhaustive search for all possible sets of these five points causes the computational time to grow exponentially with the number of edge points. For the method to be practical, the search space for the sets of five points must be reduced. This can be accomplished by means of the property of symmetry. First, the input image  $F$  is transformed into another image  $G$  by the transform procedure. Next, the nonhorizontal straight lines, for example,  $L_1, L_2, \dots, L_k$ , appearing in  $G$ , are extracted using HT. According to these lines, the proposed classification algorithm stated in the following divides  $F$  into several subimages, for example,  $f_0, f_1, f_2, \dots, f_k$ . Except for  $f_0$ , each  $f_i$  is composed of all symmetric pairs of edge points about the corresponding straight line  $L_i$ . Finally, in each subimage, all sets of five points that possibly lie on the same ellipse are located by employing the symmetry property and some geometrical properties. Note that the horizontal straight lines in  $G$  are ignored, because no ellipse will have a symmetric horizontal line produced by a rightward scan. The edge points that are not symmetric about any detected straight line are put in  $f_0$  and ignored because they cannot form an elliptical shape. The detailed classification algorithm is presented as follows.

### The classification algorithm:

```

Input:   An image F.
Output:  Several subimages of F, for example,  $f_0, f_1, f_2, \dots, f_k$ .
Step 1:  Transform  $F$  to  $G$  by the transform procedure.
Step 2:  Extract all nonhorizontal straight lines in  $G$  by the HT. If there exist such straight lines, for example,  $L_1, L_2, \dots, L_k, k \geq 1$ , then continue; otherwise, stop.

```

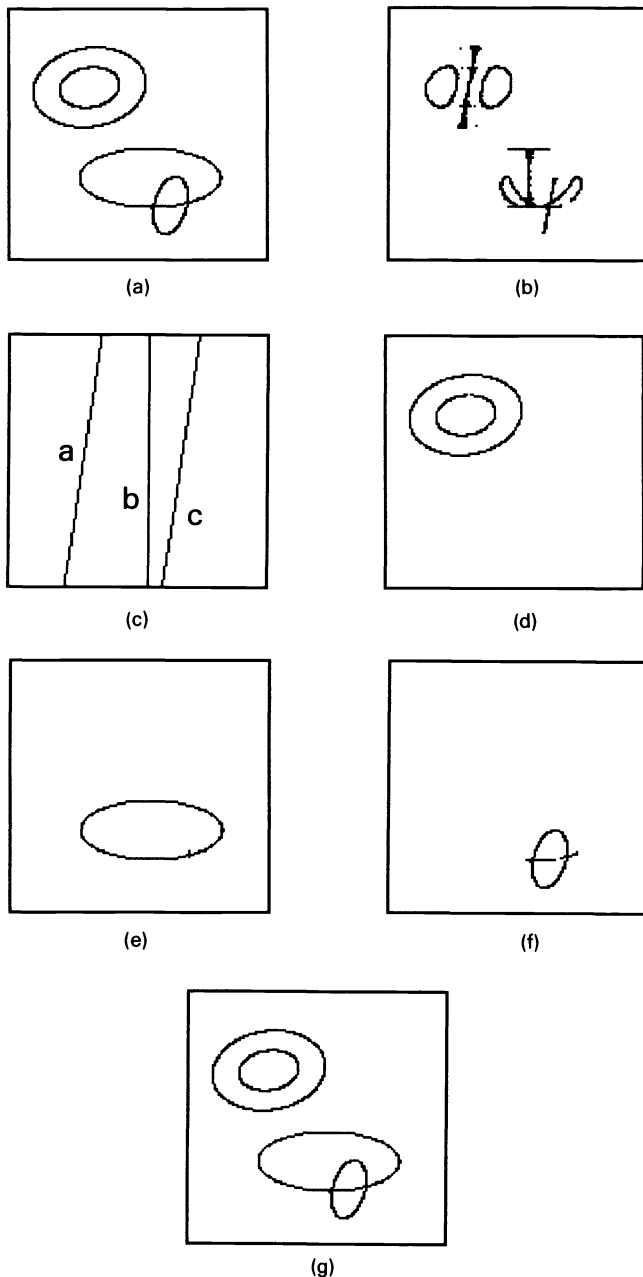


**Fig. 2** An example of a synthesized image: (a) the original image; (b) the image obtained by applying the transform procedure to (a); (c) the nonhorizontal straight lines detected in (b) and indicated as *a*, *b*, and *c*, respectively; (d) the ellipses with the same symmetric axis on line *a*; (e) the ellipse with the symmetric axis on line *b*; (f) the ellipse with the symmetric axis on line *c* and other symmetric edge points about line *c*; and (g) the final result of extracted ellipses.

**Step 3:** For each straight line  $L_i$ ,  $i = 1$  to  $k$ , locate all pairs of edge points symmetric about  $L_i$  and put them in  $f_i$ . The details are in Steps 3.1 to 3.3.

**Step 3.1:** Locate the points appearing on  $L_i$ , for example,  $m_1, m_2, \dots, m_p$ .

**Step 3.2:** Scan  $F$  and identify the pair of edge points symmetric about  $L_i$  at  $m_i$ ,  $i = 1$  to  $p$ .

**Step 3.3:** Keep all these symmetric pairs in  $f_i$ .

$$\text{Step 4: Set } f_0 = F \setminus \bigcup_{i=1}^k f_i.$$

The computational time needed for step 1 is bounded by  $O(n^3)$  and that needed for step 2 is bounded by  $O(e_G \times n)$ ; here,  $e_G$  is the number of points in  $G$ . Step 3 is bounded by  $O(e_f \times k)$ , where  $e_f$  is the average number of the edge points in each subimage. Because  $e_G$  and  $e_f$  are at most  $n^2$  and  $k$  is less than  $n$  (see Sec. 3), the total computational cost for the classification algorithm is bounded by  $O(n^3)$ .

If an ellipse exists in  $F$ , it will be classified into one of the subimages because of its symmetry. And two ellipses with different symmetric axes will be located in different subimages. This means that each subimage can be treated individually, thereby making the detection problem much easier. For example, Fig. 2(a) shows a synthesized image named image 1, which has two overlapped ellipses and two other ellipses with the same symmetric axis. The image is transformed to another image by the transform procedure [see Fig. 2(b)]. Three nonhorizontal straight lines are detected in Fig. 2(b) by the HT [see Fig. 2(c)]. The original image can be classified into three subimages [see Figs. 2(d) through 2(f)]. Each subimage contains ellipses of which the edge points are symmetric about the corresponding straight line. Note that the ellipses with the same symmetric axis are not separated by the classification algorithm [see Fig. 2(d)].

After classifying the ellipses based on their symmetric axes, the search space for the five points that lie on an ellipse can be greatly reduced. All sets of these five points are located by means of the symmetry of ellipses and some other geometrical properties, and the parameters of the determined ellipse can be estimated. The details of this process are described next.

### 2.3 Searching for the Five Candidate Points

The search for the five edge points should be conducted in an efficient way; an exhaustive search will cause a large amount of computations. In the proposed method, searching is limited to those symmetric pairs of edge points found in the same subimage, which reduces the searching space dramatically. Let  $f_i$  be the symmetric subimage about the straight line  $L_i$ . The process of selecting the five candidates consists of three procedures.

#### Procedure 1: selection of the first two candidates

First, for each pair of symmetric points  $(l, r)$ ,  $l$  is taken as the center of a  $w \times w$  window. Then, the first two candidates are each selected in turn to be the possible edge combinations, where one is at the upper-half border of the window and the other is at the lower-half border, with a restriction that the two candidates together with the center  $l$  must be allowable on the left symmetric side of an ellipse. For example, in Fig. 3 the two candidates are selected to be each of the combinations  $(a, d)$ ,  $(b, c)$ , and  $(b, d)$  in turn. But the combination of  $(a, c)$  is not considered because the candidates  $a, l$ , and  $c$  are not possible on the left symmetric side of an ellipse.

#### Procedure 2: selection of the third and fourth candidates

For each selection of the first two candidates, for example,  $l_1$  and  $l_2$ , two other candidates are selected to be  $r_1$  and  $r_2$  in

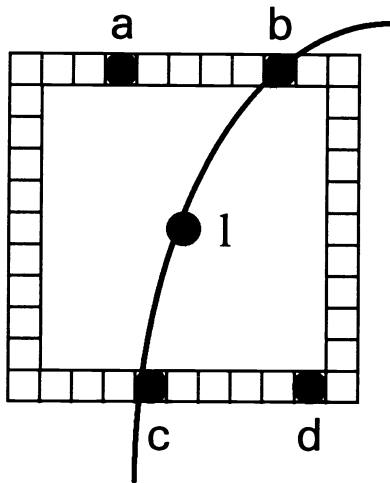


**Fig. 3** The selection of the first two candidates. The combinations  $(a, d)$ ,  $(b, c)$ , and  $(b, d)$  are selected in turn, but the combination of  $(a, c)$  is not considered because  $a$ ,  $l$ , and  $c$  are not possible on the left symmetric side of an ellipse.

which  $(l_1, r_1)$  and  $(l_2, r_2)$  are both symmetric pairs about  $L_i$ , i.e., the midpoints of  $(l_1, r_1)$  and  $(l_2, r_2)$  lie on  $L_i$ . Note that the selection of  $r_1$  and  $r_2$  does not involve any search because the symmetric information is preserved in the previous classification process.

#### Procedure 3: selection of the fifth candidate

The fifth candidate should not be selected too close to  $(l_1, l_2)$  or  $(r_1, r_2)$ ; otherwise, the quantization error will increase the inaccuracy in parameter estimation. To reduce the search space of the fifth candidate, the selection strategy is divided into two cases. One is shown in Fig. 4(a), where straight lines  $l_1l_2$  and  $r_1r_2$  intersect at a point  $R$  above the ellipse. Let  $M$  be the midpoint of  $l_1$  and  $r_1$ . The vertical straight line through  $M$  must intersect one of the straight lines  $l_1l_2$  and  $r_1r_2$  at a point, for example,  $Q$ . Then, the search path of the fifth candidate  $P_5$  is along the segment  $QM$ . Each edge point located on the segment  $QM$  is taken as the fifth candidate in turn. The other case is similar and shown in Fig. 4(b).

For each selection of the five candidates, the parameters of the determined ellipse—the ellipse center  $(x_0, y_0)$ , the half lengths of the major and minor axes  $(a, b)$ , and the rotation angle  $\theta$ —can be derived. The detailed derivation is presented in Sec. 5. By using this derived set of parameters and the concept of HT, we can extract all of the ellipses in an input image. The proposed ellipse-finding method can be summarized by the following algorithm.

#### The proposed ellipse-finding algorithm:

- Step 1: Establish an accumulator array  $A(x_0, y_0, a, b, \theta)$  and set the value of each cell to be 0.
- Step 2: Extract the edge points of an input image  $f$  and represent them by a binary image  $F$ .
- Step 3: Classify  $F$  into several subimages  $f_0, f_1, f_2, \dots, f_k$  by the classification algorithm.
- Step 4: Except  $f_0$ , for each subimage  $f_i$ ,  $i = 1$  to  $k$ , search all possible combinations of the five candidates by procedures 1 through 3 described previously.

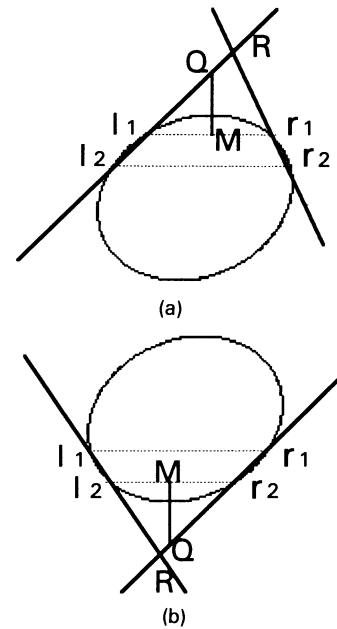


**Fig. 4** The search path  $QM$  of the fifth candidate. (a) Case 1: straight lines  $l_1l_2$  and  $r_1r_2$  intersect at a point  $R$  above the ellipse. (b) Case 2: straight lines  $l_1l_2$  and  $r_1r_2$  intersect at a point  $R$  under the ellipse.

- Step 5: For each combination of the five candidates, estimate the parameters  $(x_0, y_0, a, b, \theta)$  of a possible ellipse.
- Step 6: For each set of the estimated parameters  $(x_0, y_0, a, b, \theta)$ , increase the cell  $A(x_0, y_0, a, b, \theta)$  by 1.
- Step 7: Use a local peak detector to find all existing ellipses.

The computational cost of the proposed algorithm depends on the following factors:

- $n$  = the number of cells in each dimension of the input image  $f$
- $e_F$  = the number of points in the extracted edge image  $F$
- $e_G$  = the number of points in the resulting image  $G$  obtained by applying the transform procedure to  $F$
- $k$  = the number of subimages
- $e_f$  = the average number of edge points in each subimage
- $N_{1,2}$  = the average number of the combinations of the first two candidates  $(l_1, l_2)$  for each edge point lying on the left of a detected line
- $N_5$  = the average number of instances of the fifth candidate  $P_5$  for one combination of  $(l_1, l_2, r_1, r_2)$
- $N_{\text{map}}$  = the number of basic operations needed to transform the five candidates into the set of parameters of a possible ellipse.

Because steps 1, 2, and 7 are common to all Hough-based algorithms, we discuss only the complexity of steps 3 through

**Table 1** The experimental values of the factors.

Image name	Window size $w$	$n$	$e_F$	$e_G$	$e_f$	$k$	$N_{1,2}$	$N_5$	$N_{\text{map}}$	CPU time (seconds)
Image 1	9	128	535	552	185	3	1.79	1.29	95	1
Image 2	15	300	933	1517	528	1	0.89	3.12	95	2
Image 3	15	300	1391	4518	197	41	1.37	4.80	95	16

6, i.e., the voting stage of the HT. As mentioned above, the cost for step 3, i.e., the classification algorithm, is bound by  $O(n^3)$ . The computational time for steps 4 through 6 is bound by  $O(ke_f N_{1,2} N_5 N_{\text{map}})$ . Because  $N_{\text{map}}$  is bound by  $O(p^3)$ , and where  $p$  is the number of unknown variables in Gauss elimination,<sup>9</sup>  $p$  is equal to 5 and  $N_{\text{map}}$  approximates  $n$ . In the experiments presented in the next section,  $k$  is less than  $n$ , and  $N_{1,2}$  and  $N_5$  are very small with respect to  $n$  (see Table 1), so the computational time for steps 4 through 6 is bound by  $O(e_f n^2)$ . In total, the computation cost for steps 3 through 6 (the voting stage) is bound by  $O(e_f n^2)$ . On the other hand, the computation cost for the voting stage of the standard HT is bound by  $O(e_F n^4)$ , which is about two orders of magnitude greater than that of the proposed algorithm. Ballard's<sup>4</sup> and Huang's<sup>7</sup> methods reduce the cost to  $O(e_f n^3)$ . This is still one order of magnitude greater than that of the proposed method. Furthermore, the time  $O(n^4)$  is for the worst case of the proposed method. In the general case,  $k$  and  $e_f$  are small relative to  $n$  and  $n^2$ . The experimental results described in the next section show the effectiveness and robustness of the proposed algorithm.

### 3 Experimental Results

Several synthesized and real images have been tested on a Sony News workstation. Image 1 in Fig. 2(a) is  $128 \times 128$ . The final result is shown in Fig. 2(g). All of the ellipses are successfully extracted within 1 s.

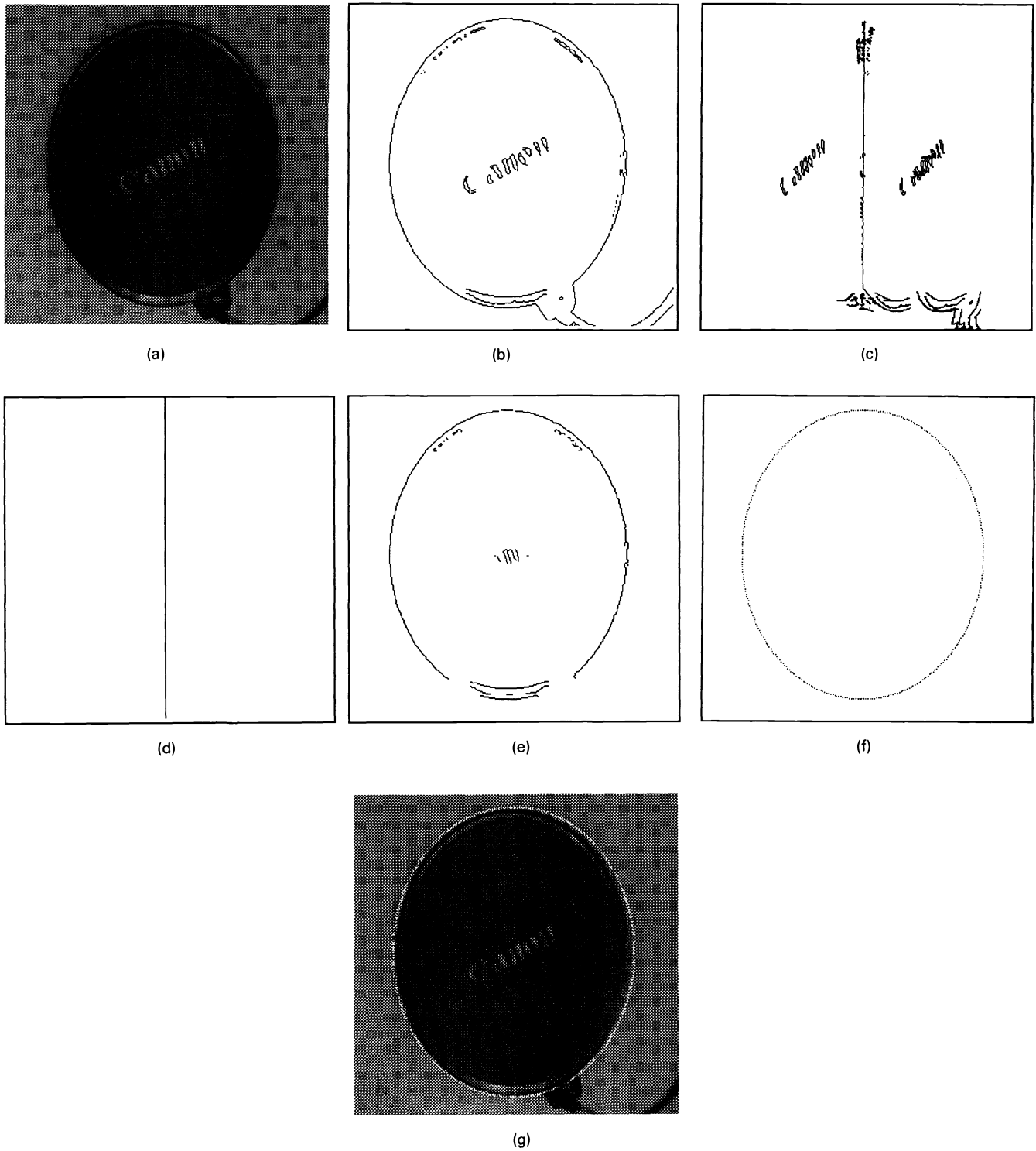
Image 2 [see Fig. 5(a)],  $300 \times 300$ , shows a real image of a lens cap. The extracted edge points of image 2 are shown in Fig. 5(b). After the transform procedure is applied, Fig. 5(b) is transformed into another image shown in Fig. 5(c). Then, the HT is applied to detect nonhorizontal straight lines, and only one straight line is detected [see Fig. 5(d)]. According to the classification algorithm, only the symmetric edge points about the detected straight line remain, as shown in Fig. 5(e). The nonsymmetric parts in the center and the lower right of Fig. 5(b) are removed because they cannot form an elliptical shape. The ellipse is extracted and superimposed on the original image [see Figs. 5(f) and 5(g)]. The CPU time required is only 2 s.

Image 3 [see Fig. 6(a)] shows a more complicated case. Many figures and lace exist in the extracted edge image [see Fig. 6(b)], which has 1391 edge points. Figure 6(c) shows the transformed result by applying the transform procedure to Fig. 6(b). Then, the HT is used to detect the nonhorizontal straight lines in Fig. 6(c). Each local peak in the accumulator array with a value greater than a certain threshold (in our

experiments, the threshold is set to be 10% of the maximum value of the accumulator array) is taken. There are 41 straight lines detected. The straight line with the maximum peak is shown in Fig. 6(d). The edge points that are symmetric about the straight line in Fig. 6(d) are shown in Fig. 6(e). Most of the edge points remain because the figures and lace are also symmetric about the straight line. Figure 6(f) shows one of the other straight lines detected in Fig. 6(c), and Fig. 6(g) shows the symmetric edge points about the straight line. Most of the edge points are not preserved in Fig. 6(g) because the straight line in Fig. 6(f) is not the real symmetric axis of the ellipses. When we apply the proposed method to all of the 41 subimages, the ellipses are extracted [see Fig. 6(h)] in 16 s and are superimposed on the original image [see Fig. 6(i)]. The ellipses cannot be extracted from many of the subimages, such as Fig. 6(g). There are three reasons for this: (1) The five-candidate combinations cannot be found in such subimages; (2) there are too few five-candidate combinations and they cannot form a peak in the accumulator array; and (3) the peak is detected, but the shape corresponding to the parameters is not matched in the input image. Consequently, only three ellipses are extracted from the 41 subimages. The experimental values of the factors mentioned in Sec. 2 are listed in Table 1. Note that  $N_{1,2}$  and  $N_5$  are very small, indicating that the search for the five candidates is very efficient.

The proposed method can be extended to detect partially occluded ellipses. Figure 7(a) shows a synthesized image including two partially occluded ellipses. Figure 7(b) shows the transformed image obtained by scanning the original image rightward. Only the symmetric axis of the right ellipse is produced. The symmetric axis of the left ellipse is not generated because the right symmetric side of the left ellipse is hidden. By adding another version of transformation, i.e., scanning the original image downward, Fig. 7(c) shows the transformed result. Both of the symmetric axes of the two ellipses are produced. Figure 7(d) shows the nonhorizontal straight line detected in Fig. 7(b), and Fig. 7(e) shows the two nonvertical straight lines detected in Fig. 7(c). Using the classification algorithm, we can classify the symmetric edge points about the straight line in Fig. 7(d) into a subimage as shown in Fig. 7(f). The symmetric edge points about the two straight lines in Fig. 7(e) are classified into two subimages as shown in Figs. 7(g) and 7(h). Finally, the three subimages in Figs. 7(f) through 7(h) are used to detect the ellipses in Fig. 7(a). The results are shown in Fig. 7(i).

The proposed method has some limitations in detecting ellipses. (1) The detected ellipses should be sufficiently complete for providing a sufficient number of symmetric pairs



**Fig. 5** The detection of ellipses in image 2: (a) image 2, (b) the extracted edge points of (a), (c) the image transformed from (b) by the transform procedure, (d) the nonhorizontal straight line detected in (c), (e) the symmetric edge points about the straight line in (d), (f) the extracted ellipse, and (g) the detected ellipse superimposed on (a).

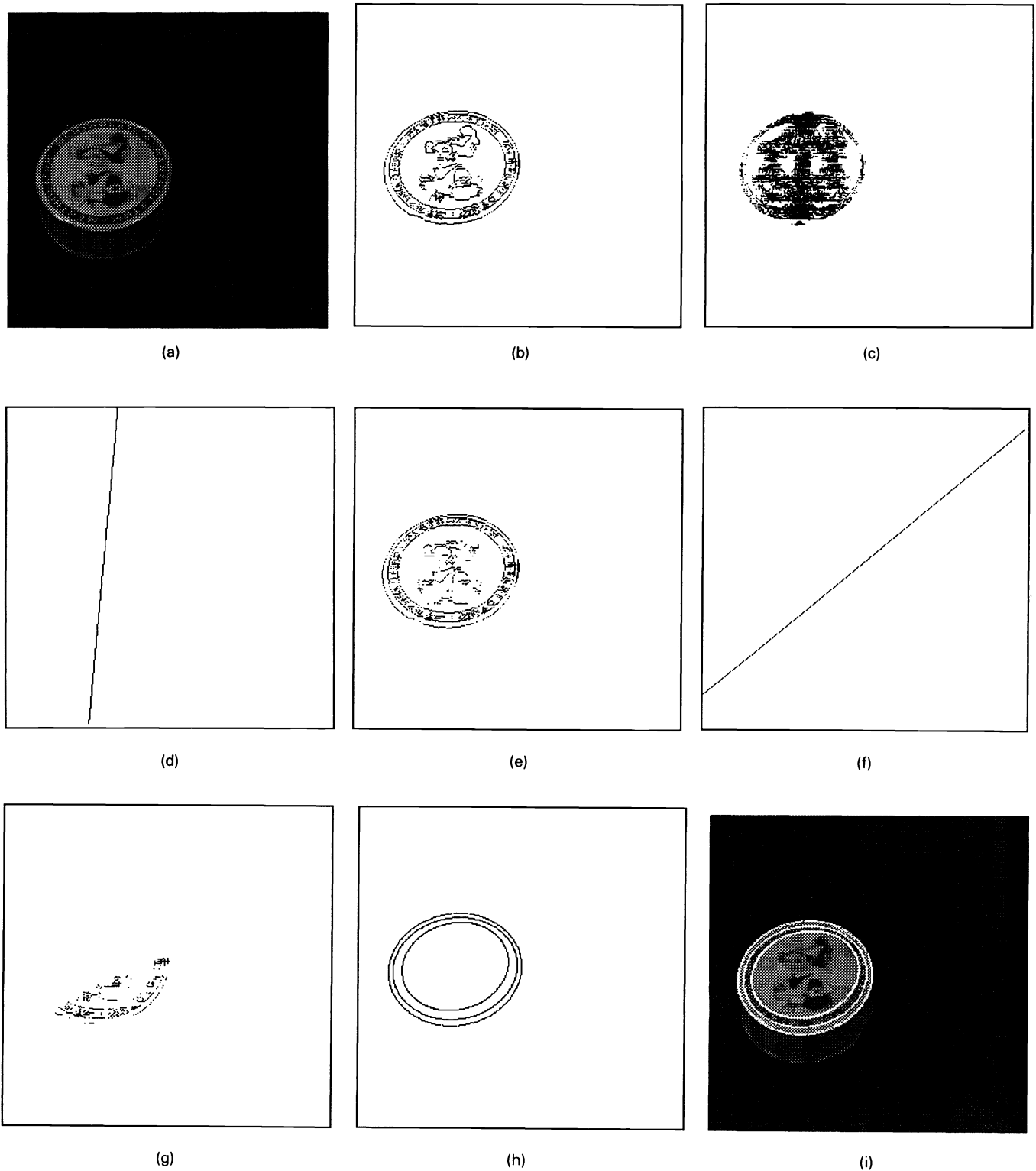


**Fig. 6** The detection of ellipses in image 3: (a) image 3, (b) the extracted edge points of (a), (c) the image transformed from (b) by the transform procedure, (d) the straight line detected with the maximum peak, (e) the edge points symmetric about the straight line in (d), (f) one of the other straight lines detected in (c), (g) the edge points symmetric about the straight line in (f), (h) the extracted ellipses, and (i) the detected ellipses superimposed on (a).

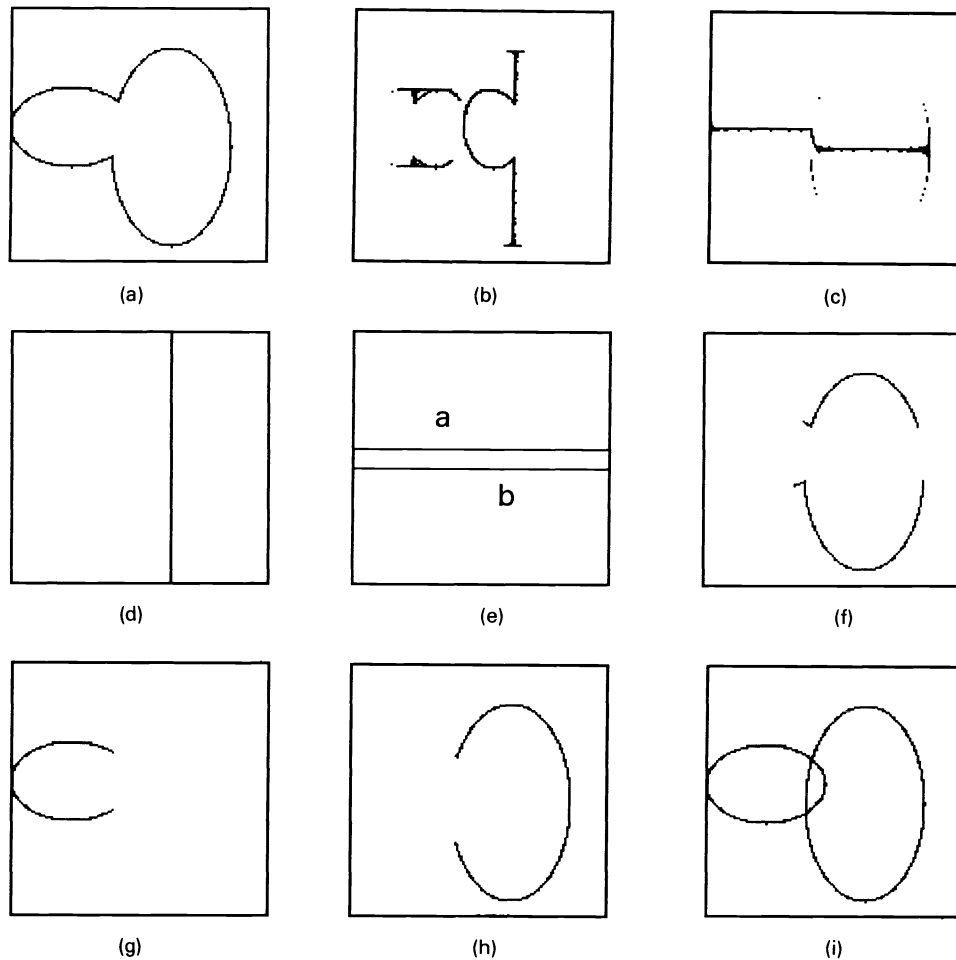


**Fig. 7** The detection of partially occluded ellipses: (a) partially occluded ellipses, (b) the image transformed from (a) by the rightward scan, (c) the image transformed from (a) by the downward scan, (d) the nonhorizontal straight line detected in (b), (e) the two nonvertical straight lines detected in (c) and indicated as *a* and *b*, (f) the symmetric subimage about the straight line in (d), (g) the symmetric subimage about the straight line *a* in (e), (h) the symmetric subimage about the straight line *b* in (e), and (i) the detected ellipses.

of edge points. (2) Some of the subimages obtained from the classification of the edge points do not contain ellipses. The computation time will increase because each subimage should be processed. (3) The length of the window side  $w$  (see procedure 1) should be selected to be no greater than the minor axes of the ellipses to be detected.

#### 4 Conclusions

In this paper, the geometrical property that five points on an ellipse can determine the parameters of the ellipse is employed to formulate a new approach for detecting ellipses. A symmetry property of ellipses is used to separate ellipses and to speed up the process of finding those five candidate points. This property can also be used to separate other symmetric shapes, such as rectangles and circles, and thus simplify the detection problem for those shapes. Furthermore, the proposed method can detect partially occluded ellipses. Experimental results show that the proposed method is effective and robust. Moreover, the gradient information is not used in the proposed method, thus reducing the inaccuracies caused by the quantization error and noise.

#### 5 Appendix

Given five distinct edge points  $P_1(x_1, y_1)$ ,  $P_2(x_2, y_2)$ ,  $P_3(x_3, y_3)$ ,  $P_4(x_4, y_4)$ , and  $P_5(x_5, y_5)$  lying on an ellipse, the parameters of the ellipse  $(x_0, y_0, a, b, \theta)$  can be derived as follows.

Consider the normal parametric form for a conic section:

$$X^2 + B_1XY + C_1Y^2 + D_1X + E_1Y + F_1 = 0 \quad (10)$$

Although Eq. (10) describes the family of ellipses, parabolas, and hyperbolas, we reject nonelliptical parameters.

First, substitute the coordinates  $(x_i, y_i)$  of the five edge points for the variables of Eq. (10) to obtain the following five equations:

$$x_1^2 + B_1x_1y_1 + C_1y_1^2 + D_1x_1 + E_1y_1 + F_1 = 0 \quad (11)$$

$$x_2^2 + B_1x_2y_2 + C_1y_2^2 + D_1x_2 + E_1y_2 + F_1 = 0 \quad (12)$$

$$x_3^2 + B_1x_3y_3 + C_1y_3^2 + D_1x_3 + E_1y_3 + F_1 = 0 \quad (13)$$

$$x_4^2 + B_1x_4y_4 + C_1y_4^2 + D_1x_4 + E_1y_4 + F_1 = 0 \quad (14)$$

$$x_5^2 + B_1x_5y_5 + C_1y_5^2 + D_1x_5 + E_1y_5 + F_1 = 0 \quad (15)$$

Then the unknown parameters  $B_1$ ,  $C_1$ ,  $D_1$ ,  $E_1$ , and  $F_1$  can be derived by Eqs. (11) through (15). To guarantee that Eq. (10) describes an ellipse,  $B_1$  and  $C_1$  must satisfy the following inequality:

$$B_1^2 - 4C_1 < 0 \quad (16)$$

otherwise, the parameters are rejected.

The rotation angle  $\theta$  can be determined by eliminating the  $XY$  term of Eq. (10) by

$$A_2X^2 + C_2Y^2 + D_2X + E_2Y + F_2 = 0 \quad (17)$$

where

$$A_2 = \cos^2\theta + B_1 \sin\theta \cos\theta + C_1 \sin^2\theta$$

$$C_2 = \sin^2\theta - B_1 \sin\theta \cos\theta + C_1 \cos^2\theta$$

$$D_2 = D_1 \cos\theta + E_1 \sin\theta$$

$$E_2 = E_1 \cos\theta - D_1 \sin\theta$$

$$F_2 = F_1$$

and

$$\theta = \frac{1}{2} \tan^{-1} \frac{B_1}{1 - C_1} \quad \text{if } C_1 \neq 1 \quad ,$$

$$= \pm \frac{\pi}{4} \quad \text{otherwise} \quad .$$

Finally, the ellipse center  $(x_0, y_0)$  and the half lengths of the major and minor axes  $(a, b)$  can be determined by

$$x_0 = \frac{-D_2}{2A_2} \quad (18)$$

$$y_0 = \frac{-E_2}{2C_2} \quad (19)$$

$$a = \left( \frac{C_2D_2^2 + A_2E_2^2 - 4A_2C_2F_2}{4A_2^2C_2} \right)^{1/2} \quad (20)$$

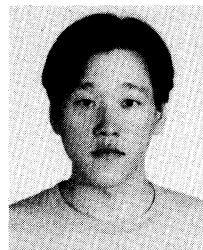
$$b = \left( \frac{C_2D_2^2 + A_2E_2^2 - 4A_2C_2F_2}{4A_2C_2^2} \right)^{1/2} \quad (21)$$

### Acknowledgment

This research was supported in part by the National Science Council of China under contract NSC-82-0408-E-009-063.

### References

1. P. V. C. Hough, "Method and means for recognizing complex patterns," U.S. Patent No. 3069654 (1962).
2. S. Tsuji and M. Matsumoto, "Detection of ellipses by a modified Hough transform," *IEEE Trans. Comput.* **27**, 777-781 (1978).
3. H. Tsukune and K. Goto, "Extracting elliptical figures from an edge vector field," in *Proc. IEEE Conf. Computer Vision and Pattern Recognition* (Washington), pp. 138-141 (1983).
4. D. H. Ballard, "Generalizing the Hough transform to detect arbitrary shapes," *Patt. Recog.* **13**, 111-122 (1981).
5. H. K. Yuen, J. Illingworth, and J. Kittler, "Detecting partially occluded ellipses using the Hough transform," *Image Vis. Comput.* **7**, 31-37 (1989).
6. J. Illingworth and J. Kittler, "The adaptive Hough transform," *IEEE Trans. Patt. Anal. Mach. Intell.* **9**, 690-698 (1987).
7. C. L. Huang, "Elliptical feature extraction via an improved Hough transform," *Patt. Recog. Lett.* **10**, 93-100 (1989).
8. R. K. K. Yip, P. K. S. Tam, and D. N. K. Leung, "Modification of Hough transform for circles and ellipses detection using a 2-D array," *Patt. Recog.* **25**, 1007-1022 (1992).
9. B. Noble and J. W. Daniel, *Applied Linear Algebra*, pp. 125-128, Prentice-Hall, N.J. (1988).



**Peng-Yeng Yin** received the BS and MS degrees in computer and information science from National Chiao Tung University, Hsinchu, Taiwan, in 1989 and 1991, respectively. Since 1991, he has been working toward his PhD degree. His current research interests include image processing, pattern recognition, and clustering.



**Ling-Hwei Chen** received the BS degree in mathematics and the MS degree in applied mathematics from National Tsing Hua University, Hsinchu, Taiwan, in 1975 and 1977, respectively, and the PhD degree in computer engineering from National Chiao Tung University, Hsinchu, Taiwan, in 1987. From August 1977 to April 1979, she worked as a research assistant at the Chung-Shan Institute of Science and Technology, Taoyan, Taiwan. From May 1979 to February 1981, she worked as a research associate in the Electronic Research and Service Organization, Industry Technology Research Institute, Hsinchu, Taiwan. From March 1981 to August 1983, she worked as an engineer in the Institute of Information Industry, Taipei, Taiwan. She joined the Department of Computer and Information Science at National Chiao Tung University in April 1987 and is currently a professor there. Her current research interests include image processing, pattern recognition, and neural networks.